Acta Cryst. (1967). **22**, 155

Propagation of Some Systematic Errors in X-ray Line Profile Analysis*

BY R. A. YOUNG, R. J. GERDES, AND A. J. C. WILSON†
Georgia Institute of Technology, Atlanta, Georgia 30332, *U.S.A.*

(*Received* 18 *February* 1966)

Three systematic errors are treated: uncorrected constant background, truncation, and the effect of sampling the observed profile at a finite number of points. Conditions under which a constant background can be ignored are presented. Background contributions to Fourier coefficients $A(n)$ for non-integer values of n generally do not vanish as they may for integer n. The use of $dA(n)/dn$ for size and strain analyses is invalidated by the presence of such background contributions as well as by truncation effects. Truncation distorts $A(n)$ values throughout the whole range of n in addition to producing a hook effect. The size distribution function, $P(n)$, is especially affected; as little as 0·5 % truncation can produce 3 % error in the average crystallite size and makes $P(1)$ negative, a physical impossibility. The use of a finite number, M, of sampling points on the observed profile makes $A(n)$ periodic in n with period M, *e.g.*, $A(M)=A(0)$. This produces an effective truncation of the $A(n)$ *versus* n curve. Investigation of this truncation provides a measure of how closely spaced the sampling points need to be in order to convey all significant profile shape information.

Introduction

The validity of X-ray line profile analyses for average values, and particularly for distributions, of crystallite size and strain depends strongly on the magnitude and nature of the errors propagated through the analyses. Important parameters are (*a*) the breadth of the intrinsic profile relative to the instrumental profile, (*b*) counting statistics and counting strategy, and (*c*) sampling factors such as estimation of the background, angular range of observation, and the number of equally spaced points at which the diffraction line intensity is actually measured. The instrumental profile is ordinarily experimentally optimized and rather inflexible for a particular instrument. The propagation of counting statistical errors and optimization of counting strategy have recently been considered (Wilson, Thomsen & Yap, 1965; Wilson, 1967). The three sampling errors mentioned are treated here.

Background corrections

Conditions under which background may be neglected

In line profile analyses a continuing problem has been the determination of the appropriate background corrections, especially in the tails of the peaks. It is shown below, however, that frequently a constant background can be ignored without significant distortion of the desired information.

In a Fourier series representation of a profile,

$$h(x) = A_0 + \sum_{\substack{-\infty \\ (n\neq 0)}}^{\infty} A_n \exp(2\pi i n x), \qquad (1)$$

A_0 is the total area under what is taken to be the net peak after background corrections, if any, have been made. Its function is to set the base line from which the represented profile will be drawn. If a constant background of intensity C, indicated in Fig. 1, is left in the data, the observed profile $h(x)=h'(x)+C$ and

$$A_n = \int_{-\frac{1}{2}}^{+\frac{1}{2}} [h'(x) + C] \exp(2\pi i n x) dx, \qquad (2)$$

which becomes

$$A_n = A'_n + C\frac{\sin \pi n}{\pi n}, \qquad (3)$$

where the primes refer to the unobserved error-free quantities. For integer n, (3) shows that only A_0 will be affected by the presence of the constant background estimation error, C. If the constant background has been overestimated C will have a negative value, thus depressing A_0 and leading to the well known 'hook' effect (*e.g.* Warren, 1959).

Since the multiplicative relation among transforms of convoluted profiles is also valid for the individual coefficients,

$$A_n^h = A_n^f A_n^g, \qquad (4)$$

where f, g, and h refer to the intrinsic, instrumental, and observed profiles, respectively. Since errors in the A_0's of $h(x)$ and $g(x)$ will affect only A_0 of $f(x)$, a constant background can be ignored when all of the significant size and strain information can be determined from the coefficients other than A_0. Criteria for ignoring A_0 can be based on the line profile results themselves, as follows.

The crystallite size distribution function, $P(n)$, is given by (Bienenstock, 1963; Smith & Simpson, 1965)

$$P(n) = \frac{A_{n+1} - 2A_n + A_{n-1}}{A_0 - A_1}. \qquad (5)$$

Here the A_n's are for the pure size broadened profile only and n is both the order number of the coefficient

* Work supported in part by the Office of Naval Research, Metallurgy Branch.

† On leave from University College, Cardiff, Wales. New permanent address: Department of Physics, The University, Birmingham 15, England.

and a measure of length, L, through the relation (Warren, 1959)

$$L=na_3'=\frac{n\lambda}{2(\sin\theta_2-\sin\theta_1)}\simeq\frac{n\lambda}{\Delta(2\theta)\cos\theta}, \qquad (6)$$

where θ_2 and θ_1 are the Bragg angles corresponding to the ends of the observation range.*

From (5), if $P(1)=0$, $A_0-A_1=A_1-A_2$. Thus if $P(1)$ is negligibly small a separate determination of the background is not needed; its inclusion in the peak measurements would distort only the unused A_0. Smith & Simpson (1965) have given a quantitative formulation of the approximations made.

While $P(1)$ cannot be determined without knowledge of the correct A_0, its relative size can be inferred in at least two ways. The size of $P(1)$ is the probability that a crystallite dimension of a_3' will occur parallel to the diffraction vector. For an extreme case such as cubes viewed parallel to a face diagonal $P(1)=P(2)=P(3)$ *etc.*, until the diagonal dimension is reached. Similarly, for cubes viewed along the body diagonal $P(1)$ would be the largest $P(n)$ of the set. But in the usual case one expects $P(1)$ to be small if a_3' is small compared to the average crystallite size, $\bar{L}$. That case can be recognized by inspection of the initial data as one may expect $a_3'\simeq\bar{L}/Q$, where Q is the ratio of the range of observation to the integral breadth of the pure size broadened profile.

The second estimate of the importance of P(1) rests on the assumption that $P(1)<P(2)$ for the usual cases (ordinary size distributions and $Q\gg1$). An unnormalized set of $P(n)$'s, excepting $P(1)$, can be derived from (5) without reference to A_0. If such a derived set shows $P(2)$ negligibly small, the assumption is that $P(1)$ will be also. Then $A_0-A_1\simeq A_1-A_2$ and the line profile analysis for size can be carried out without direct experimental determination of A_0 or the constant background. Further, these considerations of $P(1)$ can be made after the Warren & Averbach (1952) procedure, for example, has been applied to separate size and strain effect.

Graphical estimation of A_0 from the other A_n's is more readily accomplished for the pure strain broadened profile than for the size broadened profile. In certain cases discussed by Eastabrook & Wilson (1952) the strain distribution is a smoothly varying and relatively simple function, though not necessarily as simple as Gaussian.

Background contribution between integer values of n

Although for A_n restricted to integer n the constant background contributes only to A_0, it also makes a contribution between integer values of n. The use of a series representation implies a periodic function in x-space, which means that the constant background to be transformed extends in principle from minus to plus infinity. Fig. 1 indicates this situation. The Fourier transform of such a constant is $C\,\delta(n)$, which has zero value everywhere except at $n=0$. However, the transform that would actually be made in practice is that of the background rectangle of height C and unit length under a single peak. If the coordinate in transform space is t, the continuous variable version of n, the required transform is $C\sin\pi t/\pi t$, noted previously to contain all of the background contribution. While this background contribution is zero at all integer values of $t=n\neq0$, in agreement with the previous discussion of equation (3), it is distinctly not zero between integer values of n.

Fig. 2 shows the difference between continuous n and integer n as a basis for an A_n *versus* n curve. A Gaussian profile was used and the $\sin\pi n/\pi n$ contribution from an assumed constant background was included. For demonstration an unusually large value of C, 0·2, was used for Fig. 2. However, a similar plot made with $C=0{\cdot}05$ shows a disparity of nearly 3% between the two curves at $n=\frac{1}{2}$.

In the series representation, only the A_n values at integer n are defined; the slope of a single smooth curve drawn through all A_n's at points where n is

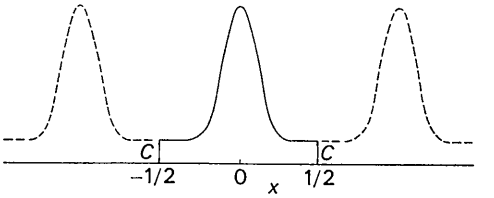

Fig. 1. Diffraction profile with a constant background, C, as represented by a Fourier series.

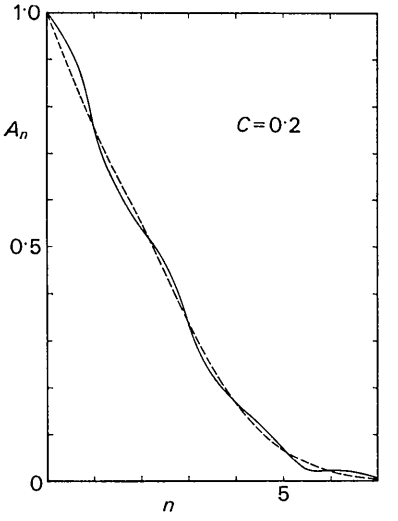

Fig. 2. Difference between continuous n (solid curve) and integer n (dashed curve) evaluations of the Fourier transform of a Gaussian profile with a constant background.

* *Note added in proof:* – There is no general reason internal to the mathematics from this point on why L cannot be arbitrarily chosen. However, in applications to actual crystals the meaning of $p(n)$ and hence the significance of equation (5) are called into question and require further discussion if the observation range does not correspond to a reciprocal lattice period (Bienenstock, 1966; Doi, 1961; and, for the equivalent problem for the strain case, Eastabrook & Wilson, 1952).

integer will not be, in general, the value of $\partial A_n/\partial n$ either at the origin, at $n=1$, at $n=2$, or at more than two intermediate points anywhere in the range $0 \le n \le 2$. These observations, then, show that valid analyses cannot be based on uncritical use of derivatives of A_n with respect to n, as has also been warned against by others (Kukol', 1962; Bienenstock, 1963; Smith & Simpson, 1965).

Inadvertent truncation from overestimation of background

In (3) and the discussion based on it there is no mathematical reason why C cannot be negative. The background can be overestimated enough to cause the apparent net intensity to fall to zero well within the observation range. In principle the appropriate negative values should be determined for the apparent net intensity over the remainder of the observation range. But in practice one assigns zeroes rather than negative intensities. The result is a truncation of the line profile data at the points where the zeroes start. Let these points be at $+B/2$ and $-B/2$ and let the range of observation be from $-R/2$ to $+R/2$. Then the second term in (3) becomes $CR\dfrac{\sin \pi nB/R}{\pi n}$, which no longer goes to zero at all integer n's but contributes errors directly to various A_n's.

Truncation effects

Truncation effects in line profile analysis have been investigated by Wilson (1942), Bertaut (1952), Eastabrook & Wilson (1952), Doi (1957), Kukol' (1962), Wilkens & Hartman (1963), and Wilson (1965), among others. A truncation necessarily occurs because the range of the observations is finite; a profile of inherently infinite extent is truncated at arbitrary points which are scaled to have coordinates $-\frac{1}{2}$ and $\frac{1}{2}$ as shown in Fig. 1. The difference between the transform of the truncated profile and the desired transform of the untruncated single profile of infinite extent can produce a 'hook' effect, and can produce serious error in the A_n's and $P(n)$'s.

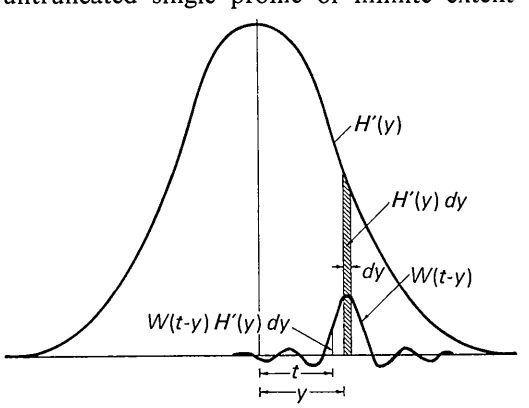

Fig. 3. Geometric representation of convolution. The function $W(t-y)$ gives a contribution at t from each element of $H'(y)$ on which it operates as indicated. The sum of such contributions from all settings of $W(t-y)$ on $H'(y)$ is the convolution, $H(t)$.

The effects of truncation may be further examined through use of the relation between convolutions and transforms. Let the observation range extend from $-R/2$ to $R/2$. Then the actual observed profile, $h(x)$, is

$$h(x)=h'(x)w(R)\,, \tag{7}$$

where $h'(x)$ is the complete profile and $w(R)$ is a window function defined as

$$w(R)=\begin{cases}1 \text{ if } -R/2 \le x \le R/2\\ 0 \text{ elsewhere}\end{cases}. \tag{8}$$

Let the transforms of $h'(x)$, $h(x)$ and $w(R)$ be $H'(t,)$ $H(t)$, and $W(t)$, respectively. By the well-known convolution theorem

$$H(t)=\int W(t-y)\,H'(y)\,dy = \int \frac{\sin \pi R(t-y)}{\pi(t-y)} H'(y)dy\,. \tag{9}$$

The action of (9) may be visualized by reference to Fig. 3. The function $W(t-y)$ operates on each element of $H'(y)$, in turn, and the successive contributions at $y=t$ are summed up by the integration. The height to which $W(t-y)$ is to be drawn depends on the factor $H'(y)dy$ and hence on its position relative to $H'(y)$. As long as $H'(y)$ is not a constant, some of the oscillatory character of $\sin \pi Rt/\pi t$ (the transform of the window function) will be present in the convolution result, $H(t)$. The degree to which this character will be apparent depends on the width of $H'(t)$ compared with, for example, $1/R$, the position of the first zero in $\sin \pi Rt/\pi t$. If $h'(x)$ is broad in relation to R, then $H'(t)$ will be narrow and the oscillatory character will be apparent. For example, let $h'(x)=\exp(-x^2/k^2)$, for which $H'(t)=(2k/\sqrt{\pi})\exp(-k^2\pi^2t^2)$. If the half-width at $1/e$ of maximum is taken as the breadth measure for the Gaussian, then the ratio of the breadth of the profile to the breadth of the observation range is k/R while that of the transforms is $R/\pi k$. The effect of increasing the observation range, R, on reducing the oscillation due to truncation of Gaussian functions is shown in Figs. 4 and 5. The figures present the starting function, the truncation points, and the individual calculations with two values of k/R corresponding to truncations at the points where the profile height has fallen to 20% and to 5% of its maximum value.

In the usual case the variables are so chosen that $R=1$. The oscillating function is then, except for a change in symbols and a scale factor, the last term of (3). But the manner of occurrence is quite different. The oscillation term in (3) is additive, hence contributes nothing at integer $t \equiv n$ and does not put the A_n's in error. The oscillatory term from truncation, being convoluted with $H(t)$ rather than added to it, does contribute errors to the A_n's.

Interest is actually in the intrinsic profile, $f'(x)$, the transform of which, $F'(t)$, is obtained from $F'(t)G'(t)=$

$H'(t)$ where $G'(t)$ is the true transform of the instrumental profile. Since $g(x)$ is ordinarily a sharp profile measured over the same range as $h(x)$, truncation effects on its transform may be neglected, at least for low and medium values of n. $F(t)$, the experimental determination of $F'(t)$, then becomes

$$F(t)=\frac{H(t)}{G(t)}=\frac{\int H'(y)\,\frac{\sin \pi R\,(t-y)}{\pi(t-y)}\,dy}{\int G'(y)\,\frac{\sin \pi R(t-y)}{\pi(t-y)}\,dy}$$

$$\simeq \frac{\int H'(y)\,\frac{\sin \pi R(t-y)}{\pi(t-y)}\,dy}{G'(t)}. \qquad (10)$$

Thus the discussion of truncation errors in $H(t)$ applies simultaneously to $F(t)$.

The effect of truncation on the general shape of $H(t)$, discussed by Bertaut (1952), Kukol' (1962) and Wilkens & Hartman (1963), is perhaps more serious than the oscillatory character. Fig. 3 shows that if the sine function is sharp, *i.e.* $R/\pi k$ is small, $H(t)$ will differ little from $H'(t)$. But if $R/\pi k$ is not small, *i.e.* if the sine function is broad relative to $H'(t)$, then $H(t)$ will be significantly broader than $H'(t)$. This broadening will have a strong effect on the slope at low values of t and, hence, on the apparent average particle size. Fig. 5 shows this feature in addition to the oscillatory character. The general effects at low values of t (or n) are a reduction (in the algebraic sense) of the curvature of $H'(t)$ near $t=0$, depression of the higher lying portions of $H'(t)$ (before renormalization) and elevation of the lower portions. Therefore, as Bertaut has pointed out, truncation can produce a 'hook' effect even in the intrinsic profile of strainfree material.

The introduction of a 'hook' and other distortion of the A_n's is shown in Fig. 6 for a case nearer to practice than is a Gaussian profile. The A_n's for an experimentally obtained profile were adjusted slightly so that the first three coefficients lay on a straight line. The modified observed profile is shown in Fig. 6(*a*). Truncations of this diffraction profile at 0·5, 5, 10 and 20% of its peak maximum resulted in the A_n *versus* n transforms shown in Fig. 6(*b*). Here each set of A_n's has been separately renormalized to $A_0=1$. A detectable 'hook' occurred even for the seemingly negligible truncation of 0·5%. Common practice in the presence of a 'hook' is to use the 'straight' portion of the A_n *versus* n curve for determination of average crystallite size. The intercept of this straight line on the ordinate is the best estimate of the true A_0. Since the true A_0 is taken to be unity, the intercept on the abscissa gives the average crystallite size directly in terms of a_3'. The effects which the various profile truncations had on the size so determined, and on the A_1/A_2 ratio, can be judged from Table 1. Truncation of a less unusual diffraction profile [Fig. 6(*c*)] resulted in even more serious errors in the determination of the average

Table 1. *Effects of various profile truncations* [*cf. Fig.* 6(*a*)]

Truncation	Change in A_1/A_2	Change in average crystallite size
0·5 %	0·05 %	3 %
5	13	20
10	26	37
20	37	140

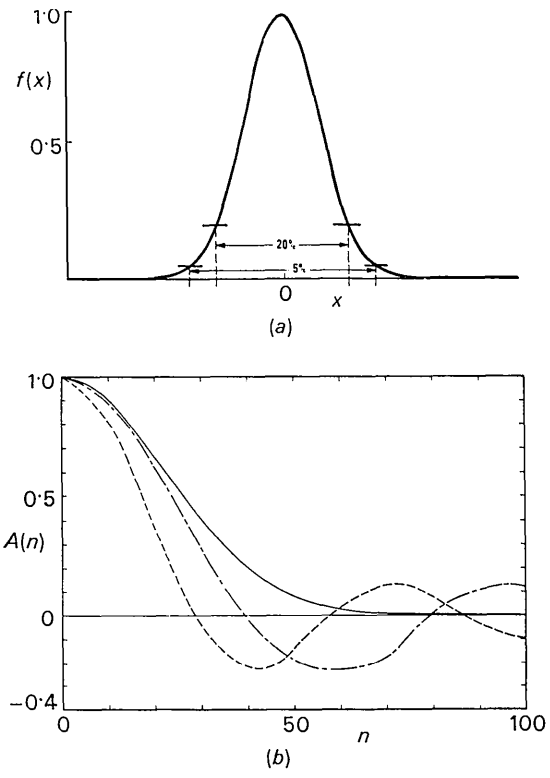

Fig. 4. (*a*) Gaussian profile with truncation points corresponding to 5 and 10 % of the peak maximum. (*b*) ——— Fourier transform of the untruncated Gaussian profile, ------ Fourier transform of the window function for the 5 % truncation case; — — — — Fourier transform of the window function for the 20 % truncation case.

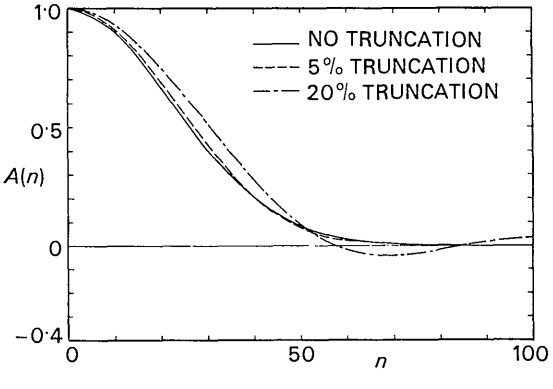

Fig. 5. Convolution of the Fourier transform of the window function with the Fourier transforms of a Gaussian for 0, 5 and 20 % truncation.

particle size (Table 2). It seems worthy of special note that a generally significant error of 20% would be made in the average crystallite size even if the truncation error were only 5%, an amount which intuitively might seem to be quite acceptable. Particularly in the case where tails of neighboring peaks overlap, as they often do for cold-worked metals, it would seem to be experimentally improbable that a truncation of less than 5% could be guaranteed.

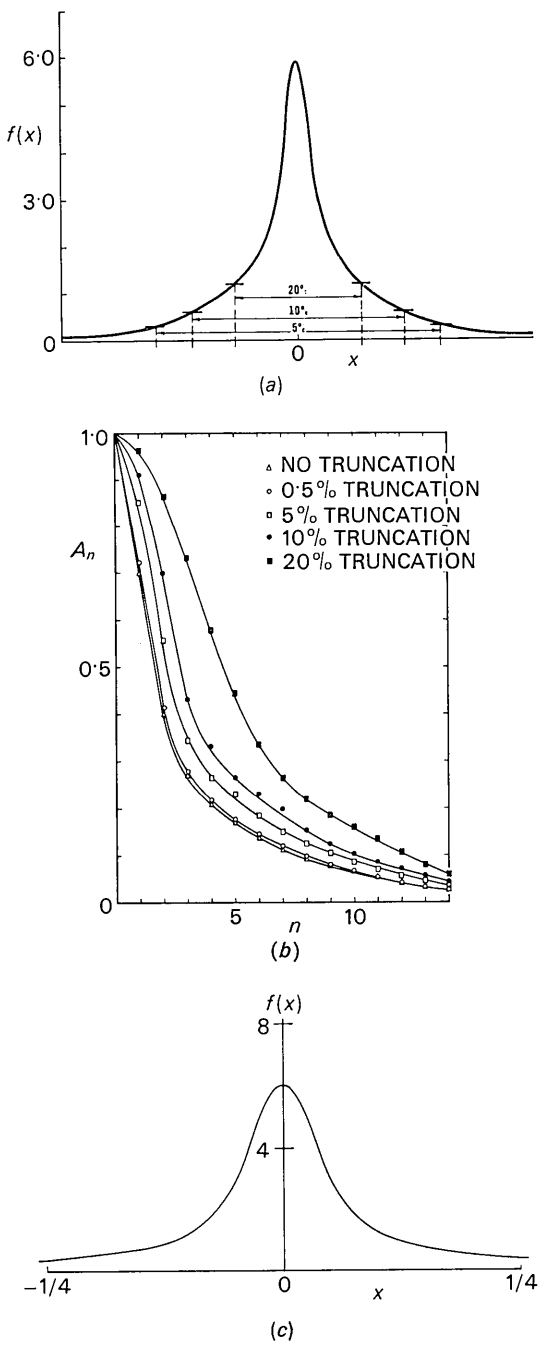

Fig. 6. (*a*) Modified observed profile and 5, 10 and 20% truncation points. (*b*) Fourier transforms of the modified diffraction profile of (*a*). (*c*) Profile used for Table 2.

Table 2. *Effects of various profile truncations [cf. Fig. 6(c)]*

Truncation	Change in A_1/A_2	Change in average crystallite size
0·5%	0·05%	5%
5	12	38
10	21	77
20	25	160

The effect of truncation on crystallite size distribution is especially marked. Fig. 7 shows the $P(n)$'s derived from equation (5) and the A_n's of Fig. 6(*b*). The general effect of truncation is to make the first $P(n)$'s smaller than they ought to be. One obvious feature of the 'hook' is the physically impossible effect of making $P(1)$ negative, as has also been noted by others, *e.g.* Bertaut (1952) and Warren (1959). Some $P(n)$'s calculated from line profile data now in the literature are shown in Fig. 8. Even though the required A_n's were obtained only from the relatively small plots published, it still appears that significant effects on the $P(n)$'s are prevalent.

Effect of finite number of profile sampling points

The validity of an A_n depends explicitly on the number of points (assumed equally spaced) at which the observed profile is sampled within the observation range. Stokes (1948) made a direct mathematical comparison

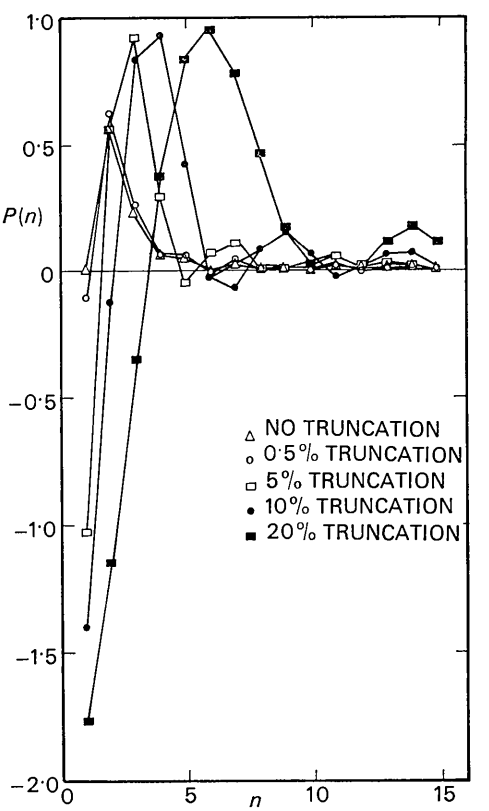

Fig. 7. Particle size distributions derived from equation (5) and the Fourier coefficients of Fig. 6(*b*).

of the expression for a profile transform as determined by integration with that determined by summation, and Doi (1957) has discussed the minimum significant spacing of sampling points as a function of experimental error and statistical fluctuation. Stokes's investigation showed that the number of sampling intervals must always exceed twice the value of n for the lowest frequency Fourier component which is effectively zero. Investigation of the same basic point by another method enlarges on this necessary, but not sufficient, condition and offers further physical understanding.

Let the observed profile height at the mth incremental position be I_m and let $A(n)$ represent a whole set of A_n's. Since the observed profile is the transform of $A(n)$ and *vice versa*, it follows that the kind of periodicity indicated in Fig. 1 is imposed on the transform in either space as a result of using incremental sampling in the other. In each case the information available is a set of coefficients (A_n or I_m) in one space which describes a periodic function in the other space. In neither case is it really the periodic function that is wanted but, rather, an untruncated non-periodic function.

To illustrate the periodic character, let the observation range, R, be divided in M parts. The choice of R determines the incremental size, relative to the characteristic features of $H(t)$, associated with an integer step in n. That $A(n)$ will have the period M in n follows from that fact that

$$A_n = \sum_{m=0}^{M} I_m \exp(2\pi i n m/M), \tag{11}$$

from which

$$A_0 = \sum_{m=0}^{M} I_m . \tag{12}$$

But

$$A_{n=M} = \sum_{m=0}^{M} I_m \exp(2\pi i M m/M) = \sum_{m=0}^{M} I_m = A_0 , \tag{13}$$

which is an absurd result for the transform of the true diffraction profile.

Since the periodicity, by constraining all non-redundant data to a finite range, introduces an effective truncation, the significance of this 'finite M effect' on the desired A_n's depends on how rapidly A_n falls to zero within the range M in n. For simple forms this comparison, in turn, depends on the breadth, β, of the observed profile relative to R/M, the sampling step size. Examples of the effect of different values of $\beta/(R/M)$ for both Cauchy and Gaussian profiles are shown in Figs. 9 through 12 for $0 \le n \le 50$. Three choices of the observation range, R, and two choices of M were used. The most obvious feature is the periodicity shown for $M=32$. By analogy with Fig. 1 and the discussion of truncation, the distortion of A_n's due to this imposition of periodicity will be negligible if the undistorted $A(n)$ has fallen to, and *remains*, effectively zero for $M/2 \le n < \infty$. The requirement that the coefficient, A_n, be effectively zero for the short wavelength components of the Fourier series representing $f(x)$ is, of course, but another way of requiring that in the observed profiles there are no significant features on a scale smaller than the step size; the actual profile is satisfactorily approximated by a series of straight lines, one for each step. That is to say, if the A_n's were transformed back to give the observed profile there would be negligible truncation error if, but only if, $A_n \simeq 0$ for $n \ge M/2$, the point in n corresponding to the end point of the observation range in Fig. 1.

For Gaussian and Cauchy profiles the conditions for negligible effect may readily be stated. Let the observation range in x-space be R, as before, and let β be the integral breadth in x-space. For the Gaussian profile,

$$f(x) = \exp(-\pi^2 x^2/\beta^2) \tag{14}$$

and

$$A(n) = \beta \exp(-\pi\beta^2 n^2/R^2) . \tag{15}$$

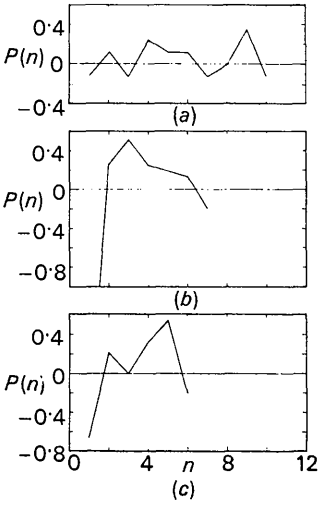

Fig. 8. Particle size distributions calculated from data of (*a*) Royen, Tolksdorf, Granzer & Schuster (1964) on magnesium oxide powder; (*b*) Warren, (1959) on cold-worked tungsten filings; (*c*) McKeehan & Warren, (1953) on thoriated tungsten filings.

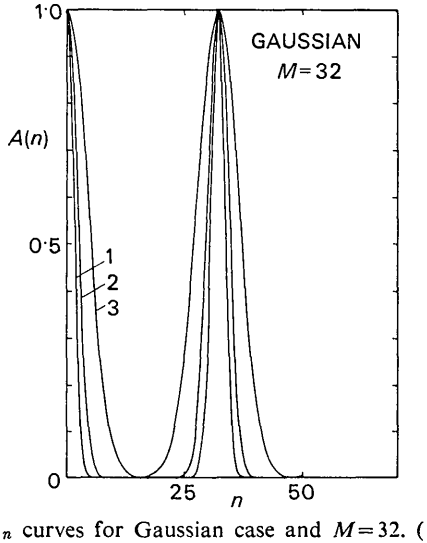

Fig. 9. A_n curves for Gaussian case and $M=32$. (1) $R=6{\cdot}4$, $\beta/(R/M)=8{\cdot}4$; (2) $R=9{\cdot}6$, $\beta/(R/M)=5{\cdot}6$; (3) $R=19{\cdot}2$, $\beta/(R/M)=2{\cdot}8$.

For the Cauchy profile,

$$f(x)=(1+\pi^2x^2/\beta^2)^{-1} \tag{16}$$

and

$$A(n)=\beta\exp(-2\beta|n|/R)\,. \tag{17}$$

Let the requirement for 'negligibly small' be that $A_n<\varepsilon A_0$ at $n=M/2$. For the Gaussian case this requires by (15) that

$$\frac{\beta}{R/M}>\frac{2}{\sqrt{\pi}}(-\ln\varepsilon)^{\frac{1}{2}} \tag{18}$$

and for the Cauchy case, by (17), that

$$\frac{\beta}{R/M}>(-\ln\varepsilon)\,. \tag{19}$$

For an example, let $\varepsilon=e^{-7}\simeq10^{-3}$. The requirement then becomes $\beta/(R/M)>3$ for the Gaussian case and >7 for the Cauchy case. (In terms of the more readily visualized width at $\frac{1}{2}$ height, instead of integral breadths, these conditions are that at least 3 or $4\frac{1}{2}$, respectively, of the sampling steps must fall within the width of the profile at half height.) The conditions for the Cauchy case of curve 3 of Fig. 11, for example, did not meet this requirement; the conditions for curve 2 do, just, as there $\beta/(R/M)=6{\cdot}7\simeq7$. Curve 3 of Fig. 9 is an example of a Gaussian case in which the above step-size requirement is barely met.

The reason that the requirements on $\beta/(R/M)$ turned out to be so relatively undemanding in these examples is that both Cauchy and Gaussian profiles are smoothly varying functions which do not show much small-scale character. One would anticipate that actual experimental profiles might have much more small-scale character that should be preserved, and the minimum acceptable value of $\beta/(R/M)$ should be substantially increased accordingly.

In any event, actual carrying out of the transforms to $n\geq M/2$ will provide direct evidence of whether a sufficiently small step-size was used. If A_n does not fall effectively to zero before n reaches $M/2$ a smaller step-size is needed. If A_n falls to zero only for n quite close to $M/2$, the step size should be decreased (M increased) to assure that no significant oscillations in A_n *versus* n are being omitted by the unavoidable truncation at $n=M/2$. Conversely, if A_n falls effectively to zero for $n\ll M/2$ and remains there, as n increases, an unnecessarily small step size is being used.

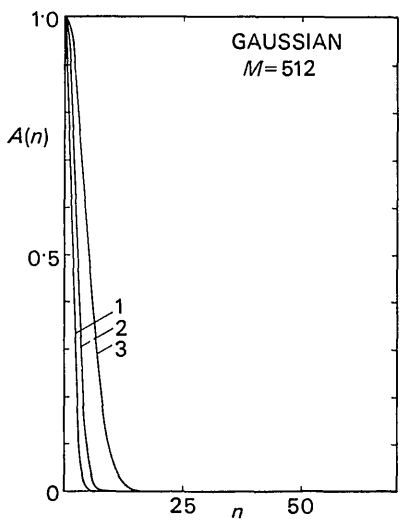

Fig. 10. A_n curves for same Gaussian case as Fig. 9 but with $M=512$. (1) $R=6{\cdot}4$, $\beta/(R/M)=134$; (2) $R=9{\cdot}6$, $\beta/(R/M)=89$; (3) $R=19{\cdot}2$, $\beta/(R/M)=45$.

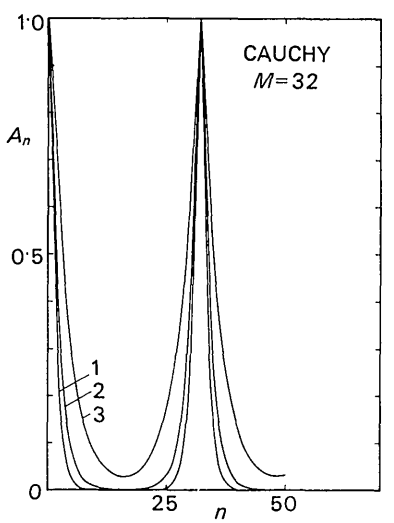

Fig. 11. A_n curves for Cauchy case with $M=32$. (1) $R=6{\cdot}4$, $\beta/(R/M)=10$; (2) $R=9{\cdot}6$, $\beta/(R/M)=6{\cdot}7$; (3) $R=19{\cdot}2$, $\beta/(R/M)=3{\cdot}3$.

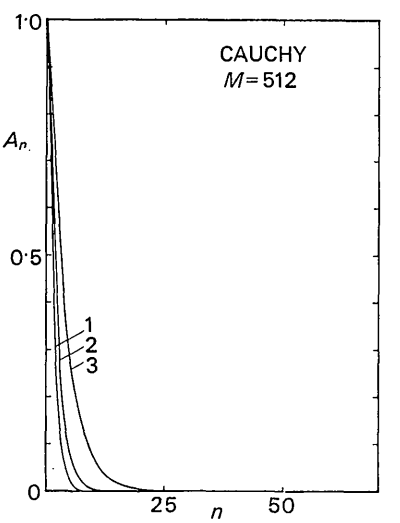

Fig. 12. A_n curves for same Cauchy case as Fig. 11 but with $M=512$. (1) $R=6{\cdot}4$, $\beta/(R/M)=160$; (2) $R=9{\cdot}6$, $\beta/(R/M)=106{\cdot}7$; (3) $R=19{\cdot}2$, $\beta/(R/M)=53{\cdot}3$.

References

Bertaut, E. F. (1952). *Acta Cryst.* **5**, 117.
Bienenstock, A. (1963). *J. Appl. Phys.* **34**, 1391.
Bienenstock, A. (1966). Private communication.
Doi, K. (1957). *Bull. Soc. franç. Minér. Crist.* **80**, 325.

DOI, K. (1961). *Acta Cryst.* **14**, 830.
EASTABROOK, J. N. & WILSON, A. J. C. (1952). *Proc. Phys. Soc.* B**65**, 67.
KUKOL', V. V. (1962). *Fizika Tverdogo Tela,* **4**, 724.
MCKEEHAN, M. & WARREN, B. E. (1953). *J. Appl. Phys.* **24**, 52.
ROYEN, P., TOLKSDORF, W., GRANZER, F. & SCHUSTER, H. (1964). *Acta Cryst.* **17**, 1246.
SMITH, V. H., JR. & SIMPSON, P. G. (1965). *J. Appl. Phys.* **36**, 3285.
STOKES, A. R. (1948). *Proc. Phys. Soc.* B**61**, 382.
WARREN, B. E. (1959). *Progr. Metal Phys.* **8**, 147.
WARREN, B. E. & AVERBACH, B. L. (1952). *J. Appl. Phys.* **23**, 497.
WILKENS, M. & HARTMAN, R. J. (1963). *Z. Metallk.* **54**, 676.
WILSON, A. J. C. (1942). *Proc. Royal Soc.* A, **180**, 277.
WILSON, A. J. C. (1965). *Proc. Phys. Soc.* **85**, 807.
WILSON, A. J. C. (1967). In preparation.
WILSON, A. J. C., THOMSEN, J. C. & YAP, F. Y. (1965). *Appl. Phys. Letters,* **7**, 163.

Acta Cryst. (1967). **22**, 162

The Structures of Zeolite Sorption Complexes. I. The Structures of Dehydrated Zeolite 5A and its Iodine Sorption Complex*

BY KARL SEFF† AND DAVID P. SHOEMAKER

Department of Chemistry and Center for Materials Science and Engineering, Massachusetts Institute of Technology, Cambridge, Massachusetts 02139, *U.S.A.*

(*Received* 10 *January* 1966 *and in revised form* 13 *June* 1966)

The structure of dehydrated synthetic zeolite 5A ($Ca_4Na_4Al_{12}Si_{12}O_{48}$, cubic, $Pm3m$, $a_0 = 12{\cdot}42 \pm 0{\cdot}01$ Å) has been refined by least-squares analysis of X-ray powder diffraction data, and the structure of its sorption complex with nearly six iodine molecules per unit cell ($Ca_4Na_4Al_{12}O_{48}.5.65I_2$, $a_0 = 12{\cdot}29 \pm 0{\cdot}07$ Å) has been determined and similarly refined. In the 'empty' dehydrated zeolite the two kinds of cation appear to have somewhat different positions on the threefold axes, the Ca^{2+} ion being close to the plane of the 6-ring oxygen window of the sodalite unit and the Na^+ ion being displaced about 0·4 Å inward from that position into the sodalite unit. Si,Al–O framework distances are 1·63–1·69 Å. In the iodine sorption complex, the I_2 molecules lie in mirror planes of the framework structure; they are near the large windows and tipped at 32·5° to the window planes. The relative orientations of I_2 molecules could not, however, be completely determined. The I_2 molecules in one unit cell have a maximum possible aggregate point symmetry $\bar{3}$ and the overall structure is presumably disordered. Two different arrangements with point symmetry $\bar{3}$ are possible, and are regarded as more probable than some less symmetrical arrangements. The I_2 interatomic distance uncorrected for thermal motion is 2·72 Å, in fair agreement with the value 2·68 Å reported for solid iodine; the corrected value, 2·79 Å, may be in significant excess of reported values of about 2·67 Å for gaseous I_2 molecules. Each I_2 molecule makes close approaches in its axial direction to a framework oxygen atom and to an iodine atom in an adjacent molecule, with an I···O distance of 3·29 Å and an I···I distance of 3·46 Å. The latter, and a non-axial I···I contact distance of 4·01 Å, compare roughly with analogous distances of 3·54 Å and 4·06 Å in solid iodine.

Introduction

This is one of several papers from this laboratory that will deal with zeolite 'inclusion complexes' or 'sorption complexes'; that is, zeolites containing sorbed molecules of various kinds. The object of work of this kind is to determine the positions of sorbed molecules in relation to the structure of the substrate sorber; *i.e.* the sorption sites on the internal 'surface' of the zeolite pores. In this and the following papers the zeolite is the synthetic type A, selected on account of its relative simplicity of structure, its stability to dehydration, and its capability of sorbing a variety of small molecules. In particular, most of the work will deal with '5A' zeolite, which as a result of partial calcium exchange contains fewer cations than '4A' and consequently has a somewhat greater sorption capability.

The present paper deals with the refinement of the structure of the 'empty' (dehydrated) 5A zeolite and the determination of the positions at which iodine molecules, I_2, are sorbed. A related paper, based on prior work done in this laboratory on a bromine sorption complex of 4A zeolite, is being published elsewhere

* This work was supported by the Army Research Office (Durham). Computations were carried out in part by the M.I.T. Computation Center.

† This work was done in partial fulfilment of the requirement for the degree of Doctor of Philosophy. Present address: Department of Chemistry, University of California, Los Angeles 24, California.